Microscope Observation of Morphology of Colloidally Dispersed Niobate Nanosheets Combined with Optical Trapping

Teruyuki Nakato,[ab] Yuki Higashi,[c] Wataru Ishitobi,[a] Takashi Nagashita,[c] Makoto Tominaga,[c]† Yasutaka Suzuki[c], Toshiaki Iwai,[d] and Jun Kawamata*[c]*

[a] Department of Applied Chemistry, Kyushu Institute of Technology, 1-1 Sensui-cho, Tobata, Kitakyushu, Fukuoka 804-8550, Japan.

[b] Strategic Research Unit for Innovative Multiscale Materials, Kyushu Institute of Technology, 1-1 Sensui-cho, Tobata, Kitakyushu, Fukuoka 804-8550, Japan.

[c] Graduate School of Sciences and Technology for Innovation, Yamaguchi University, 1677-1 Yoshida, Yamaguchi, Yamaguchi 753-8512, Japan.

[d] Graduate School of Bio-Applications and Systems Engineering, Tokyo University of Agriculture and Technology, 2-24-16 Naka-cho, Koganei, Tokyo 184-8588, Japan.

Abstract

Although inorganic nanosheets prepared by exfoliation (delamination) of layered crystals have attracted great attention as 2D nanoparticles, in situ real space observations of exfoliated nanosheets in colloidally dispersed state have not been conducted. In the present study, colloidally dispersed inorganic nanosheets prepared by exfoliation of layered niobate are directly observed with bright-field optical microscopy, which detects large nanosheets with lateral length larger than several micrometers. The observed nanosheets are not strictly flat but rounded, undulated, or folded in many cases. Optical trapping of nanosheets by a laser radiation pressure clarified their uneven cross-sectional shapes. Their morphology is retained under the relation between Brownian motion and optical trapping

INTRODUCTION

Inorganic nanosheets prepared by exfoliation (delamination)[1] of layered crystals such as various ion-exchangeable oxides, graphite, metal chalcogenides, and transition metal carbides/nitrides (MXenes) have attracted great attention due to their potential broad applications based on their extreme thinness and high 2D shape anisotropy.[2-5] They are obtained as colloidally dispersed particles through exfoliation in solvents in many cases. Whereas their transfer to a flat substrate results in deposition of flat particles reflecting the 2D shape,[6, 7] wrinkled, scrolled and irregularly shaped particles are obtained under other conditions of solvent removal.[8-15] Understanding of accurate nanosheet shape in colloidal state with direct observation

is indispensable in order to further develop and more precisely control the structures of nanosheet assemblies.

However, the real shape of "as exfoliated" nanosheets before the solvent removal has scarcely been observed directly yet. Two-dimensional morphology of exfoliated nanosheets in colloidally dispersed states has been supported by several methods. Phase transition of nanosheet colloids to lyotropic liquid crystals nanosheets[15-24] evidences 2D morphology of exfoliated nanosheets because the phase behavior of nanosheet colloids agrees with the phase transition theory that assumes a disk-like particle shape.[25, 26] Small-angle scattering studies demonstrate disk-like morphology of various nanosheets in colloidal states based on a power-law relationship between scattering vector and intensity.[18, 27-29] On the other hand, combined neutron and X-ray scattering at an ultra-small-angle region for colloidal niobate nanosheets prepared from single-crystalline hexaniobate $K_4Nb_6O_{17}$ indicates formation of a fractal structure in colloids.[29] The fractal structure strongly suggests the presence of undulated nanosheets when their lateral size is larger than the persistence length of the structure. Undulation and bending of nanosheets in their colloidally dispersed state is possible because of their thinness (~ 1 nm) even though they retain two-dimensionality in the colloid.

In the present study, we have succeeded in observing large single nanosheets of exfoliated hexaniobate dispersed in an aqueous colloid by an optical microscope. Our recent report indicated optical microscope observations of exfoliated niobate nanosheets[30] in a colloidal liquid crystalline state.[19] In that study, an optical microscope with the spatial resolution of ~ 1 μm was employed for optical manipulation[31] of nanosheets by a tightly focused laser beam. Optical manipulation has been used for trapping various colloidal particles.[32-38] The optical microscope

system used for the laser trapping possesses almost the same spatial resolution as the diffraction limit. It will therefore be employable to observe individual colloidal nanosheets. We have attempted to observe single nanosheets with their lateral sizes of several micrometers in a dilute isotropic colloid. In addition, optical trapping of nanosheets has been carried out to observe their cross-sectional morphologies through pinning and aligning each nanosheet in the colloid. Various irregularly shaped, such as undulated, bent, and rounded, nanosheets are frequently observed as well as rigidly flat platy particles. All the particles are completely exfoliated and thus not multi-layered. An important finding is the stability of distorted particle morphology as evidenced by the retention of the particle shape under the relation between the Brownian motion and trapping by the focused laser beam.

EXPERIMENTAL SECTION

Sample preparation. A colloidal sample of niobate nanosheets was prepared by the method reported previously. Single crystalline particles of tetrapotassium hexaniobate $K_4Nb_6O_{17}$ prepared by a flux method. The size of each single crystalline particles was about 1 mm thickness and several mm width. The single crystalline particles were collected, and treated with a 0.2 mol L^{-1} aqueous propylammonium chloride ($C_3H_7NH_3Cl$) solution at 120 °C for a week in a Teflon-lined stainless steel autoclave. Then, solid product was centrifuged, washed and dialyzed with water to yield the initial stock colloid sample. With these treatments, the layered niobate crystals were exfoliated to form of colloidal niobate nanosheets. The average lateral length of the nanosheets estimated by TEM images was 5.5 μm with a log-normal size distribution (Figure S1, Supporting Information). The purified nanosheets were finally dispersed in water to yield

the stock colloidal sample of niobate nanosheets. The nanosheet concentration of the stock sample was 0.01 g L^{-1} (based on the mass of $K_4Nb_6O_{17}$).

Microscope observation. A small portion of sample was injected into a 100-μm thick thin-layer glass cell. The cell was set on the stage of an inverted microscope (IX70, Olympus) equipped with a water-immersion objective lens (UPlanSApo, Olympus, 60×, N.A. = 1.20). The band-limited light is selected by a band-pass filter (410 ± 80 nm) from the white light emitted from the halogen lamp attached to the microscope. The microscopic bright-field movies were recorded as 12-bit grayscale images with a digital CMOS camera (ORCA-Flash 4.0 V3, Hamamatsu Photonics). Spatial resolutions in this setup was experimentally determined to be around 1 μm.

Optical trapping. The experimental setup is shown in Figure 1. A linearly polarized CW Gaussian laser beam that emitted at 532 nm (Millennia Pro, Spectra Physics) was guided to the optical microscope, and focused at the center of the cell (50 μm from the cell surface) by the objective lens of microscope. The laser power was set to 20 mW at the exit pupil of the objective lens. We confirmed that the laser beam was blocked completely by a dichroic mirror and the band pass filter that was inserted before the camera.

RESULTS AND DISCUSSION

Our optical setup (Figure 1) successfully detects single niobate nanosheets with their lateral size larger than around 3 μm in a colloidally dispersed state. Figure 2 shows microscope snapshot images extracted from movies of various colloidal nanosheets moving in the colloid

with schematic drawings of their morphology. Although all of the particles are essentially recognized as 2D sheets, many nanosheets suffer from distortion to some extent. Typical examples of flat and deformed nanosheets are indicated in Figure 2; we classified the deformed nanosheets into rounded, undulated, and folded ones based on their edge shape as defined in Figure S2 (Supporting Information). By sampling nanosheets randomly in the microscope images, the fractions of flat and deformed nanosheets are estimated as 40% and 60%, respectively, as shown in Figure 3.

Full movies are shown in Movies 1–5 (Supporting Information). All of the movies show random walk of the platy particles, which confirms the observed objects as nanosheets colloidally dispersed in the solvent (water). The movies also demonstrate that the colloidal nanosheets retain their deformed morphology during Brownian motion.

Individual particles detected by the optical microscope are judged as single nanosheets because they are very thin and homogeneous. Folding and scrolling into multilayers are not observed. Also, overlapping and stepping are not found on the sheet surfaces, which denies stacking of more than two nanosheets. The thickness of observed particles (~ 2 μm) apparently much larger than the crystallographic thickness of hexaniobate nanosheets (~ 1.6 nm)[10, 39, 9, 40] is rationalized by blurring of the objects at the edges due to defocusing based on optical geometry (Figure S3, Supporting Information). These nanosheet shapes are consistent with the result of previous small-angle scattering study, which reports existence of a mass-fractal structure in niobate nanosheet colloids on the basis of scattering power-law at a low q region.[29] This structure assumes undulation of nanosheets when their lateral lengths are larger than the persistence length of the structure being several micrometers.

Randomly moving nanosheets are trapped and aligned by the focused laser beam in the colloid, which enables selective microscope observations of cross sections of nanosheets. Our recent optical manipulation study of niobate nanosheets has clarified that colloidally dispersed niobate nanosheets are trapped at the focal point of linearly polarized laser beam and oriented with their in-plane direction parallel to the propagation direction of the incident laser beam, and that the nanosheets are also aligned with their edge (longitudinal) direction in parallel to the polarization direction of the incident irradiation, i.e., optical electric field of the linearly polarized incident laser beam.[30, 41] The biaxial alignment leads to unidirectional orientation of colloidal nanosheets.

Such trapping is also the case for colloidal niobate nanosheets examined in the present study. Figure 4 shows microscope snapshot images extracted from movies of single nanosheets of niobate with various shapes under the illumination of the linearly polarized laser beam. Full movies are shown in Movies 6–10 (Supporting Information). They demonstrate trapping of nanosheets by the focused laser beam. When a single nanosheet randomly walking in the colloid reaches the focal point of the incident laser beam, it is trapped as evidenced by the suppression of particle translation. The trapped nanosheet is rotated, and aligned parallel to the propagation direction of the laser beam. With this nanosheet alignment, we unambiguously observe the cross-sectional morphology of each nanosheet. This state is kept for several tens of seconds in our observation conditions. Subsequently, the nanosheet is swept away along the direction of incident laser beam, and becomes unobservable by the optical microscope.

As shown in Figure 2, most of nanosheets indicate cross sections deviated from straight line to some extent by reflecting the deformation from rigidly flat nanosheet morphology. They are somewhat rounded, undulated, or, folded as mentioned above. In most cases, the trapped nanosheets are aligned with their edges in parallel to the polarization direction as well as the light

propagation direction, as mentioned above (Figures 4a and d and Movies 6 and 9, Supporting Information). Folded nanosheets are aligned with one of the folded edges in parallel to the polarization direction (Figure 4e and Movie 10, Supporting Information). Rounded nanosheets are trapped at a point on their arced edge, but direction of the rest parts of the edge is not determined strictly (Figures 4b and c and Movies 7 and 8, Supporting Information). This is rationalized by the beam waist size (~ 1 μm) at the focal point that is much smaller than the nanosheet edge length, and their round shapes that allow trapping at only a single point on the arced edge.

A striking discovery is retention of various deformed morphology of niobate nanosheets under the irradiation of the laser beam. The deformed nanosheets are rotated, aligned, and diffuse away with retaining their shapes involving curvatures and folding angles. A rare exception is partly cracked nanosheets observed in a very few cases, and these nanosheets undergo folding along the crack under the laser beam (Figure 5 and Movie 11, Supporting Information).

These results indicate that the deformed morphologies of niobate nanosheets are basically stable against radiation pressure of the focused laser beam and hydrodynamic forces applied during the diffusion and rotation of nanosheets. In other words, nanosheets suffer from stresses stronger than these external forces in their deformation process, and the deformed morphologies are retained under relatively weak forces applied with both the Brownian and laser-induced motions. Such strong stresses would be applied during the exfoliation of niobate crystals. Because the crystal structure of niobate is realized by strong electrostatic interactions between the anionic niobate nanosheets via interlayer cations, strong energies must be injected to cleave the layer stacking and exfoliate individual nanosheets. This condition is fulfilled by the

intercalation of exfoliating reagent (propylammonium ions), which expands the interlayer space and entrains water molecules there, and the propylammonium ions stay on the exfoliated anionic nanosheets as counter cations.[42] In such an exfoliation process of layered niobate, however, exfoliating reagent is not quantitatively intercalated.[43] This can lead to inhomogeneous distribution of propylammonium ions on nanosheet surfaces, and thus inhomogeneous application of stresses to nanosheets to cause morphological deformations.

Another finding of the present study is the absence of deeply crumpled or scrolled nanosheets even though undulated, bent, and rounded nanosheets are present. Crumpling has been reported for various nanosheets, and recognized as an important morphological transformation for applying nanosheets to various functional materials.[44] However, deeply crumpled nanosheets have been observed usually in solid state after the removal of solvents although stabilization of the crumpled state in solvents has been reported. A recent study of crumpled graphene oxide nanosheets has indicated relaxation of crumpling in solvents through swelling, dissociation, and stretching.[45] The absence of deeply crumpled niobate nanosheets in our colloidal sample clearly demonstrates that as exfoliated nanosheets in solvents are not crumpled without specific treatments.

CONCLUSIONS

In conclusion, niobate nanosheets with large lateral lengths obtained by exfoliation of hexaniobate layered crystals are directly observed with bright-field optical microscopy in a colloidally dispersed state. Although platy morphologies of nanosheets are unambiguously indicated, they are not strictly flat but deformed to some extent into various shapes such as

undulated, bent, folded, or rounded in many cases. The nanosheet deformation confirms the prediction by our small-angle scattering study on undulated morphology of niobate nanosheets with lateral length longer than the persistence length of the fractal structure of nanosheet colloids. The deformed morphology is stable against Brownian motion and optical trapping by the laser radiation pressure. Although the optical microscope can detect nanosheets with the lateral sizes larger than several micrometers, our result is the first example of directly observing exfoliated nanosheets in colloidal state under Brownian motion and optical trapping. The present results unravel the real shape of the colloidally dispersed nanosheets and will be used as most fundamental knowledge in materials chemistry of inorganic nanosheets.

ASSOCIATED CONTENT

Supporting Information.

TEM image and lateral size distribution of nanosheets, illustration of nanosheet shape classification, and illustration of blurring of a nanosheet edge (PDF).

Movies 1-5 show Brownian motion of nanosheets (AVI).

Movies 6-11 show optical trapping of nanosheets (AVI).

AUTHOR INFORMATION

Corresponding Author

*E-mail: nakato@che.kyutech.ac.jp (T. N.).

*E-mail: j_kawa@cc.yamaguchi-u.ac.jp (J. K.).

Present Addresses

†Department of Inorganic Chemistry I, University of Bayreuth, Universitätsstraße 30, Bayreuth, 95447, Germany.

Author Contributions

The manuscript was written through contributions of all authors. All authors have given approval to the final version of the manuscript.

ACKNOWLEDGMENT

This work was financially supported by JSPS KAKENHI Grant Numbers 16K14095 (for T.N.) and 17H05466 (for Y.S.).

REFERENCES

(1) Whereas the term “exfoliation” is generally used for indicating disassembly or liberation of unit layers from inorganic layered crystals, the term “delamination” is also used. Differences in the usage of these two terms are not clear in published articles, although some researchers provided different definitions for these terms (for example, Gardolinski, J. E. F. C.; Lagaly, G., *Clay Miner*., **2005**, *40*, 547-556). However, because such a definition has not been widely accepted at present, we use the term “exfoliation” in this report.

(2) Nakato, T.; Kawamata, J.; Takagi, S., *Inorganic Nanosheets and Nanosheet-Based Materials*. Springer: Tokyo, 2017.

(3) Osada, M.; Sasaki, T., Two-Dimensional Dielectric Nanosheets: Novel Nanoelectronics from Nanocrystal Building Blocks. *Adv. Mater.* **2012,** *24*, 210-28.

(4) Eigler, S.; Hirsch, A., Chemistry with Graphene and Graphene Oxide-Challenges for Synthetic Chemists. *Angew. Chem. Int. Ed.* **2014,** *53*, 7720-38.

(5) Bhimanapati, G. R.; Lin, Z.; Meunier, V.; Jung, Y.; Cha, J.; Das, S.; Xiao, D.; Son, Y.; Strano, M. S.; Cooper, V. R.; Liang, L. B.; Louie, S. G.; Ringe, E.; Zhou, W.; Kim, S. S.; Naik, R. R.; Sumpter, B. G.; Terrones, H.; Xia, F. N.; Wang, Y. L.; Zhu, J.; Akinwande, D.; Alem, N.; Schuller, J. A.; Schaak, R. E.; Terrones, M.; Robinson, J. A., Recent Advances in Two-Dimensional Materials Beyond Graphene. *ACS Nano* **2015,** *9*, 11509-11539.

(6) Keller, S. W.; Kim, H.-N.; Mallouk, T. E., Layer-by-Layer Assembly of Intercalation Compounds and Heterostructures on Surfaces: Toward Molecular "Beaker" Epitaxy. *J. Am. Chem. Soc.* **1994,** *116*, 8817-8818.

(7) Kleinfeld, E. R.; Ferguson, G. S., Stepwise Formation of Multilayered Nanostructural Films from Macromolecular Precursors. *Science* **1994,** *265*, 370-373.

(8) Abe, R.; Shinohara, K.; Tanaka, A.; Hara, M.; Kondo, J. N.; Domen, K., Preparation of Porous Niobium Oxides by Soft-Chemical Process and Their Photocatalytic Activity. *Chem. Mater.* **1997,** *9*, 2179-2184.

(9) Saupe, G. B.; Waraksa, C. C.; Kim, H.-N.; Han, Y. J.; Kaschak, D. M.; Skinner, D. M.; Mallouk, T. E., Nanoscale Tubles Formed by Exfoliation of Potassium Hexaniobate. *Chem. Mater.* **2000,** *12*, 1556-1562.

(10) Miyamoto, N.; Kuroda, K., Preparation of Porous Solids Composed of Layered Niobate Walls from Colloidal Mixtures of Niobate Nanosheets and Polystyrene Spheres. *J. Colloid Interface Sci*. **2007,** *313*, 369-373.

(11) Nabetani, Y.; Takamura, H.; Hayasaka, Y.; Shimada, T.; Takagi, S.; Tachibana, H.; Masui, D.; Tong, Z.; Inoue, H., A Photoactivated Artificial Muscle Model Unit: Reversible, Photoinduced Sliding of Nanosheets. *J. Am. Chem. Soc*. **2011,** *133*, 17130-17133.

(12) Guo, F.; Kim, F.; Han, T. H.; Shenoy, V. B.; Huang, J.; Hurt, R. H., Hydration-Responsive Folding and Unfolding in Graphene Oxide Liquid Crystal Phases. *ACS Nano* **2011,** *5*, 8019-8025.

(13) Bastakoti, B. P.; Li, Y.; Imura, M.; Miyamoto, N.; Nakato, T.; Sasaki, T.; Yamauchi, Y., Polymeric Micelle Assembly with Inorganic Nanosheets for Construction of Mesoporous Architectures with Crystallized Walls. *Angew. Chem. Int. Ed*. **2015,** *54*, 4222-5.

(14) Sun, L.; Ying, Y.; Huang, H.; Song, Z.; Mao, Y.; Xu, Z.; Peng, X., Ultrafast Molecule Separation through Layered WS_2 Nanosheet Membranes. *ACS Nano* **2014,** *8*, 6304-6311.

(15) Xia, Y.; Mathis, T. S.; Zhao, M. Q.; Anasori, B.; Dang, A.; Zhou, Z.; Cho, H.; Gogotsi, Y.; Yang, S., Thickness-Independent Capacitance of Vertically Aligned Liquid-Crystalline MXenes. *Nature* **2018,** *557*, 409-412.

(16) Gabriel, J.-C. P.; Davidson, P., Mineral Liquid Crystals from Self-Assembly of Anisotropic Nanosystems. *Top. Curr. Chem*. **2003,** *226*, 119-172.

(17) Nakato, T.; Miyamoto, N., Liquid Crystalline Behavior and Related Properties of Colloidal Systems of Inorganic Oxide Nanosheets. *Materials* **2009,** *2*, 1734-1761.

(18) Gabriel, J.-C. P.; Camerel, F.; Lemaire, B. J.; Desvaux, H.; Davidson, P.; Batail, P., Swollen Liquid-Crystalline Lameller Phase Based on Extended Solid-Like Sheets. *Nature* **2001,** *413*, 504-508.

(19) Miyamoto, N.; Nakato, T., Liquid Crystalline Nature of $K_4Nb_6O_{17}$ Nanosheet Sols and Their Macroscopic Alignment. *Adv. Mater.* **2002,** *14*, 1267-1270.

(20) Michot, L. J.; Bihannic, I.; Maddi, S.; Funari, S. S.; Baravian, C.; Levitz, P.; Davidson, P., Liquid–Crystalline Aqueous Clay Suspensions. *Proc. Natl. Acad. Sci. USA* **2006,** *103*, 16101-16104.

(21) Behabtu, N.; Lomeda, J. R.; Green, M. J.; Higginbotham, A. L.; Sinitskii, A.; Kosynkin, D. V.; Tsentalovich, D.; Parra-Vasquez, A. N. G.; Schmidt, J.; Kesselman, E.; Cohen, Y.; Talmon, Y.; Tour, J. M.; Pasquali, M., Spontaneous High-Concentration Dispersions and Liquid Crystals of Graphene. *Nat. Nanotechnol.* **2010,** *5*, 406-411.

(22) Xu, Z.; Gao, C., Graphene Chiral Liquid Crystals and Macroscopic Assembled Fibres. *Nat. Commun.* **2011,** *2*, 571.

(23) Mejia, A.; Chang, Y.-W.; Ng, R.; Shuai, M.; Mannan, M.; Cheng, Z., Aspect Ratio and Polydispersity Dependence of Isotropic-Nematic Transition in Discotic Suspensions. *Phys. Rev. E* **2012,** *85*, 061708-1-061708-12.

(24) Wong, M.; Ishige, R.; Hoshino, T.; Hawkins, S.; Li, P.; Takahara, A.; Sue, H.-J., Solution Processable Iridescent Self-Assembled Nanoplatelets with Finely Tunable Interlayer Distances Using Charge- and Sterically Stabilizing Oligomeric Polyoxyalkyleneamine Surfactants. *Chem. Mater.* **2014,** *26*, 1528-1537.

(25) Onsager, L., The Effects of Shape on the Interaction of Colloidal Particles. *Ann. N. Y. Acad. Sci.* **1949,** *51*, 627-659.

(26) Vroege, G. J.; Lekkerkerker, H. N. W., Phase Transitions in Lyotropic Colloidal and Polymer Liquid Crystals. *Rep. Prog. Phys.* **1992,** *55*, 1241-1309.

(27) Kroon, M.; Vos, W. L.; Wegdam, G. H., Structure and Formation of a Gel of Colloidal Disks. *Phys. Rev. E* **1998,** *57*, 1962-1970.

(28) Ramsay, J. D. F.; Linder, P., Small-Angle Neutron Scattering Investigations of the Structure of Thixotropic Dispersions of Smectite Clay Colloids. *J. Chem. Soc., Faraday Trans.* **1993,** *89*, 4207-4214.

(29) Yamaguchi, D.; Miyamoto, N.; Koizumi, S.; Nakato, T.; Hashimoto, T., Hierarchical Structure of Niobate Nanosheets in Aqueous Solution. *J. Appl. Crystallogr.* **2007,** *40*, s101-s105.

(30) Tominaga, M.; Nagashita, T.; Kumamoto, T.; Higashi, Y.; Iwai, T.; Nakato, T.; Suzuki, Y.; Kawamata, J., Radiation Pressure Induced Hierarchical Structure of Liquid Crystalline Inorganic Nanosheets. *ACS Photonics* **2018,** *5*, 1288-1293.

(31) Ashkin, A., Acceleration and Trapping of Particles by Radiation Pressure. *Phys. Rev. Lett.* **1970,** *24*, 156-159.

(32) Ashkin, A.; Dziedzic, J. M.; Bjorkholm, J. E.; Chu, S., Observation of a Single-Beam Gradient Force Optical Trap for Dielectric Particles. *Opt. Lett.* **1986,** *11*, 288-290.

(33) Misawa, H.; Koshioka, M.; Sasaki, K.; Kitamura, N.; Masuhara, H., Three-Dimensional Optical Trapping and Laser Ablation of a Single Polymer Latex Particle in Water. *J. Appl. Phys.* **1991,** *70*, 3829-3836.

(34) Svoboda, K.; Block, S. M., Optical Trapping of Metallic Rayleigh Particles. *Opt. Lett.* **1994,** *19*, 930-932.

(35) Tan, S.; Lopez, H. A.; Cai, C. W.; Zhang, Y., Optical Trapping of Single-Walled Carbon Nanotubes. *Nano Lett.* **2004,** *4*, 1415-1419.

(36) Inaba, K.; Imaizumi, K.; Katayama, K.; Ichimiya, M.; Ashida, M.; Iida, T.; Ishihara, H.; Itoh, T., Optical Manipulation of Cucl Nanoparticles under an Excitonic Resonance Condition in Superfluid Helium. *Phys. Stat. Sol. B* **2006,** *243*, 3829-3833.

(37) Neves, A. A. R.; Camposeo, A.; Pagliara, S.; Saija, R.; Borghese, F.; Denti, P.; Iatì, M. A.; Cingolani, R.; Maragò, O. M.; Pisignano, D., Rotational Dynamics of Optically Trapped Nanofibers. *Opt. Express* **2010,** *18*, 822-830.

(38) Tong, L.; Miljković, V. D.; Käll, M., Alignment, Rotation, and Spinning of Single Plasmonic Nanoparticles and Nanowires Using Polarization Dependent Optical Forces. *Nano Lett.* **2010,** *10*, 268-73.

(39) Exfoliation of hexaniobate $K_4Nb_6O_{17}$ yields bilayer nanosheets where every other interlayer space is cleaved due to the layered structure of hexaniobate characterized by alternative presence of two structurally different interlayer spaces.

(40) Nakato, T.; Sakamoto, D.; Kuroda, K.; Kato, C., Synthesis of Two Types of Intercalation Compounds of Potassium Niobate ($K_4Nb_6O_{17}$) with Tris(2,2'-Bipyridyl) Metal Complex Ions. *Bull. Chem. Soc. Jpn.* **1992,** *65*, 322-8.

(41) Tominaga, M.; Higashi, Y.; Kumamoto, T.; Nagashita, T.; Nakato, T.; Suzuki, Y.; Kawamata, J., Optical Trapping and Orientation Manipulation of 2D Inorganic Materials Using a Linearly Polarized Laser Beam. *Clays Clay Miner.* **2018,** *66*, 138-145.

(42) Miyamoto, N.; Nakato, T., Liquid Crystalline Colloidal System Obtained by Mixing Niobate and Aluminosilicate Nanosheets: A Spectroscopic Study Using a Probe Dye. *Langmuir* **2003,** *19*, 8057-8064.

(43) Nakato, T.; Miyamoto, N.; Harada, A.; Ushiki, H., Sol-Gel Transition of Niobium Oxide Nanosheet Colloids: Hierarchical Aspect of a Novel Macroscopic Property Appearing in Colloidally Dispersed States of Layered Niobate $K_4Nb_6O_{17}$. *Langmuir* **2003,** *19*, 3157-3163.

(44) Dou, X.; Koltonow, A. R.; He, X.; Jang, H. D.; Wang, Q.; Chung, Y. W.; Huang, J., Self-Dispersed Crumpled Graphene Balls in Oil for Friction and Wear Reduction. *Proc. Natl. Acad. Sci. USA* **2016,** *113*, 1528-1533.

(45) Chen, C.; Xu, Z.; Han, Y.; Sun, H.; Gao, C., Redissolution of Flower-Shaped Graphene Oxide Powder with High Density. *ACS Appl. Mater. Interfaces* **2016,** *8*, 8000-8007.

Figures captions

Figure 1. Experimental setup for the optical microscope observations and optical manipulation by laser irradiation.

Figure 2. Microscope images of single (a) flat, (b) and (c) rounded, (d) undulated, and (e) folded nanosheets of hexaniobate in the colloidally dispersed state and schematic drawings of their morphology.

Figure 3. Variation of the shapes of niobate nanosheets. The nanosheet shapes were classified into flat, rounded, undulated, and folded (see Figure S1, Supporting Information), and the fraction of each shape was estimated from 200 nanosheets more than 5 μm of lateral length observed in the optical microscope images.

Figure 4. Microscope images (snapshots) of single (a) flat, (b) and (c) rounded, (d) undulated, and (e) folded nanosheets of hexaniobate with various shapes before and under the irradiation of linearly polarized laser beam. The single-headed white arrows point the focusing point of the laser beam, and the double-headed yellow arrows indicate the polarized direction of the laser beam.

Figure 5. Microscope images (snapshots) of a cracked nanosheet of hexaniobate before and after the irradiation of linearly polarized laser beam, and schematic drawings of their morphology. The single-headed white arrows point the focusing point of the laser beam, and the double-headed yellow arrows indicate the polarized direction of the laser beam.

Figures

Figure 1

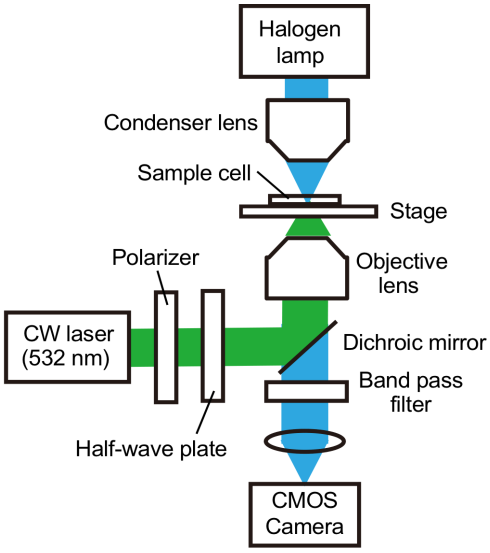

Figure 2.

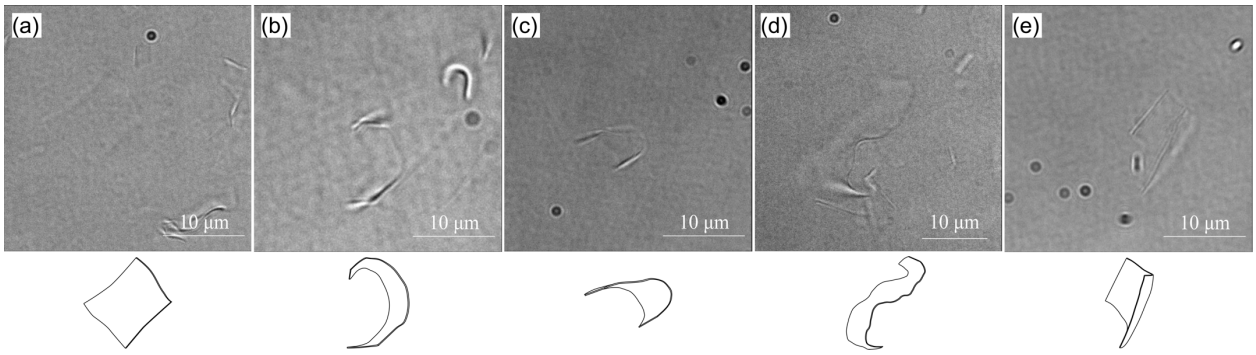

Figure 3.

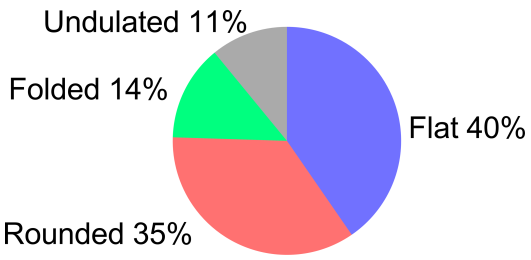

Figure 4.

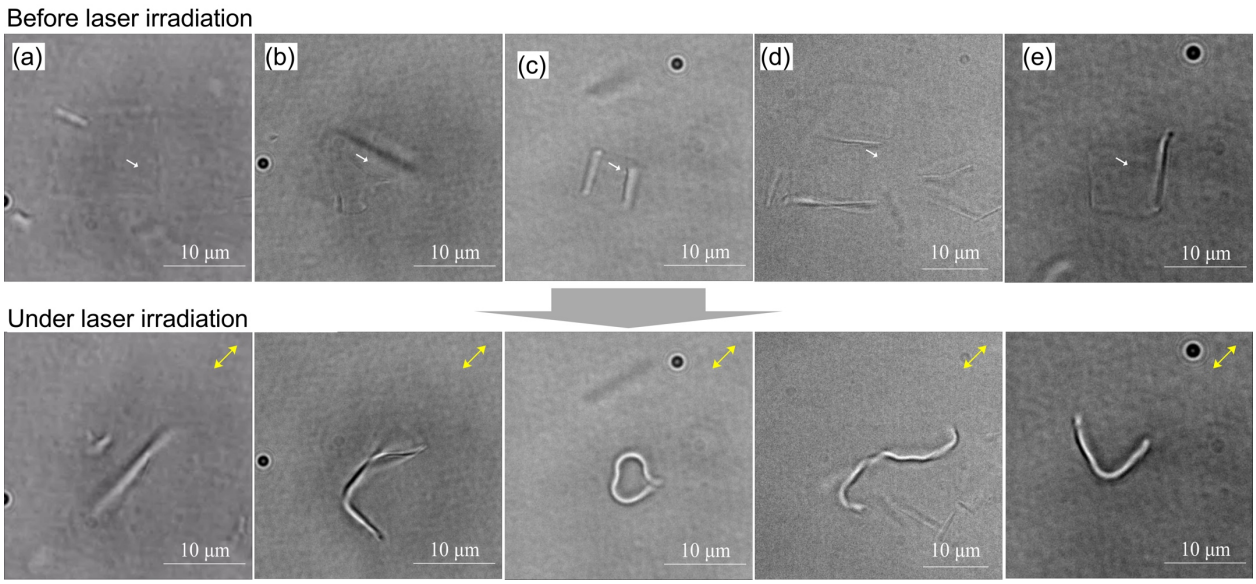

Figure 5.

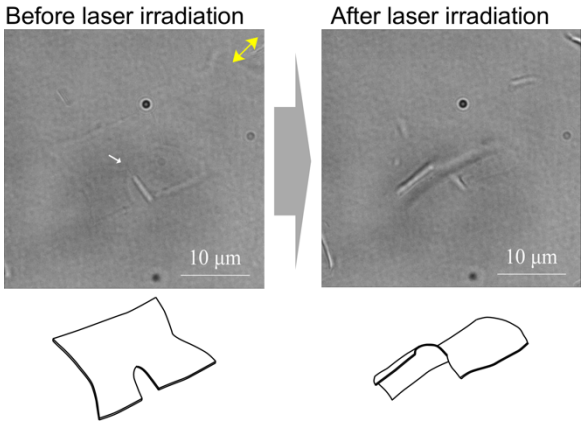
Before laser irradiation
After laser irradiation
10 μm
10 μm

For Table of Contents Use Only